

Vibrational and Rotational Excitation of Molecular Hydrogen by Electron Impact

Ronald J. W. Henry

Department of Physics and Astronomy, Louisiana State University, Baton Rouge, Louisiana 70803

(Received 22 April 1970)

The close-coupling approximation is used to calculate integral and differential cross sections for pure vibrational excitation $\sigma(v=0 \rightarrow 1, \Delta j=0)$ and $\sigma(v=0 \rightarrow 2, \Delta j=0)$, and for simultaneous rotational-vibrational excitation $\sigma(v=0 \rightarrow 1, \Delta j=2)$ of H_2 by slow-electron impact. Static-field and electron-exchange effects, long-range quadrupole, and an effective polarization potential are included in the $e-H_2$ interaction. Pure vibrational cross sections are found to depend on the initial rotational state j of the molecule, but the total vibrational cross section is almost independent of j . Cross sections are compared with experiments for energies $E \leq 10$ eV. For $2 < E < 5$ eV, $\sigma(v=0 \rightarrow 1, \Delta j=0)$ and $\sigma(v=0 \rightarrow 1, j=1 \rightarrow 3)$ are 50% larger than experimental values while agreement is better in the remaining energy regions. For $1 < E < 3$ eV, $\sigma(v=0 \rightarrow 2, \Delta j=0)$ is in good agreement with experiment but is underestimated for $E > 3$ eV. Differential scattering cross sections for vibrational excitation are found to be dominated by the polarization potential at low angles, and by the short-range potential at large angles.

I. INTRODUCTION

In this paper, we present calculations for integral and differential cross sections for pure vibrational excitation $\sigma(v=0 \rightarrow 1, \Delta j=0)$ and $\sigma(v=0 \rightarrow 2, \Delta j=0)$, and for simultaneous rotational excitation $\sigma(v=0 \rightarrow 1, \Delta j=2)$ of the ground electronic state of molecular hydrogen by electrons with energies $E \leq 10$ eV.

An early theoretical investigation¹ of vibrational excitation of H_2 by electron impact yielded values for the cross section which were much smaller than those obtained from experiment. Carson¹ used the Born approximation and included only short-range interactions between the electron and the molecule. Takayanagi² used the polarized Born approximation in his study of the relative importance of various parts of the interaction potential, and found that the symmetric portion of the polarization force is most important. This gives a long-range term in the potential and it arises from the interaction of an incident electron with the induced dipole moment of the molecule. When a potential of this type is used, the resulting cross section has a magnitude comparable to experimental data.

A knowledge of the variation of the interaction potential with internuclear separation is required in order to calculate vibrational-excitation cross sections. Breig and Lin³ used Raman intensity data to determine this variation and they investigated a number of approximations for the short-range cutoff parameter for the polarization potential. Truhlar *et al.*⁴ performed calculations in

the polarized Born and Born-Ochkur-Rudge approximations. They extended the work of Breig and Lin to include, in the potential, contributions from long-range quadrupole and polarization terms and from short-range interactions.

Bardsley *et al.*,⁵ and Abram and Herzenberg,⁶ using a different approach, obtained results which are in fair agreement with experiment for both integral and differential cross sections. They assumed that the $e-H_2$ interaction can be described in terms of a resonance between the electron and the molecular potential. In this model, an electron is trapped in a temporary negative-ion state of H_2^- , and potential energy curves for this state are constructed from experimental data on the position of the resonance.

This single-particle resonant state occurs because the electron is trapped by a combination of polarization, exchange, static-field and centrifugal-barrier effects. We will attempt to incorporate all these effects in the $e-H_2$ interaction potential.

The theory discussed in Sec. II is based on the work of Ardill and Davison⁷ who generalized the scattering formalism of Arthurs and Dalgarno.⁸ We have extended this treatment to include vibrational excitation in a manner similar to that given by Massey.⁹ The short-range and long-range interaction potentials, given in Sec. III, are then used in a close-coupling calculation. The importance of static, short-range, and polarization effects on pure vibrational excitation of H_2 by electron impact is discussed in Sec. IV, where integral and differential cross sections for total vi-

brational and simultaneous rotational-vibrational excitation are compared with experiment. The principal conclusions are summarized in Sec. V.

II. *e*-H₂ SCATTERING THEORY

In the adiabatic approximation, the wave function for the ground electronic state of molecular hydrogen may be given by

$$\Phi = \phi_0(\vec{r}_1, \vec{r}_2, \vec{s}) Z(vj|s), \quad (1)$$

where the electronic wave function ϕ_0 satisfies

$$[T_e + U_e(\vec{r}_1, \vec{r}_2, \vec{s}) - \epsilon(s)]\phi_0(\vec{r}_1, \vec{r}_2, \vec{s}) = 0 \quad (2)$$

and the vibrational-rotational wave function Z satisfies

$$[T_n + \epsilon(s) - E_{vj}]Z(vj|s) = 0, \quad (3)$$

where v and j represent the vibrational and rotational quantum numbers, respectively. The potential U_e denotes the Coulomb interaction of all particles; \vec{r}_1 and \vec{r}_2 are the electronic coordinates with respect to the midpoint of the nuclei, \vec{s} is the vector joining the two nuclei; T_e and T_n are the electronic and nuclear kinetic-energy operators, respectively, given by

$$T_e = -\frac{1}{2}(\nabla_1^2 + \nabla_2^2), \quad T_n = -(1/2\mu)\nabla_s^2. \quad (4)$$

The wave equation for a system of an electron colliding with molecular hydrogen may be written (we shall use atomic units throughout)

$$[T_e + T_n - \frac{1}{2}\nabla_3^2 - E - E_{vj} + U_e + V(\vec{r}_1, \vec{r}_2, \vec{r}_3; \vec{s})]\Psi = 0, \quad (5)$$

where $V(\vec{r}_1, \vec{r}_2, \vec{r}_3; \vec{s})$ is the potential energy of the interaction of the incident electron with the nuclei and with the molecular electrons; \vec{r}_3 is the coordinate of the colliding electron with respect to the midpoint of the nuclei; E_{vj} and E are the energies of the initial state of the molecule and the kinetic energy of the incident electron, respectively.

We may expand the total wave function in the form

$$\Psi = \sum_{1,2,3} \phi_0(\vec{r}_1, \vec{r}_2, \vec{s}) \Lambda(\vec{r}_3, \vec{s}) \chi(1, 2; 3), \quad (6)$$

where the summation is over cyclic interchanges of electrons, and $\chi(1, 2; 3)$ is the doublet spin function.

Substitute Eq. (6) into Eq. (5), use Eq. (2), multiply by $\phi_0(\vec{r}_1, \vec{r}_2, \vec{s}) \chi^\dagger(1, 2; 3)$, integrate over $d\vec{r}_1 d\vec{r}_2$, and sum over spin, and we obtain

$$\begin{aligned} & [\frac{1}{2}\nabla_3^2 - (T_n + \langle \phi_0 | T_n | \phi_0 \rangle) + E + E_{vj} - \epsilon(s) \\ & - \iint V(\vec{r}_1, \vec{r}_2, \vec{r}_3; \vec{s}) |\phi_0(\vec{r}_1, \vec{r}_2, \vec{s})|^2 d\vec{r}_1 d\vec{r}_2] \Lambda(\vec{r}_3, \vec{s}) \\ & + (\text{exchange terms}) = 0. \end{aligned} \quad (7)$$

Let

$$\Lambda(\vec{r}_3, \vec{s}) = \sum_{\alpha''} F_{\alpha''}(\vec{r}_3, \vec{s}) Z(v''j''|s), \quad (8)$$

where

$$F_{\alpha''}(\vec{r}_3, \vec{s}) = r_3^{-1} u_{\alpha''}^J(r_3) \mathcal{Y}_{Jj''}^{M''}(\hat{r}_3, \vec{s}). \quad (9)$$

Here $u_{\alpha''}^J(r_3)$ are the radial functions which describe the motion of the colliding electron, $\alpha \equiv vjl$, and the angular momentum l of the colliding electron is coupled with j to form J , the total angular momentum of the system. The quantum numbers J and $M = m_j + m_l$ represent the magnitude and component of J along the z axis. The angular basis functions are the eigenfunctions of J^2 and J_z and are given by

$$\mathcal{Y}_{Jj}^M(\hat{r}_3, \vec{s}) = \sum_{m_j m_l} C(jlJ; m_j m_l M) Y_{j m_j}(\hat{s}) Y_{l m_l}(\hat{r}_3), \quad (10)$$

where $C(jlJ; m_j m_l M)$ are Clebsch-Gordan coefficients, and $Y_{j m_j}$ are spherical harmonics.

Substitute Eqs. (8) and (9) into (7), use Eq. (3), multiply by $\mathcal{Y}_{Jj}^{M*}(\hat{r}_3, \vec{s}) Z(v'j'|s)$, and integrate over $d\vec{s} d\hat{r}_3$, and we obtain a set of coupled equations for the radial functions u , which may be written

$$\begin{aligned} & \left(\frac{d^2}{dr_3^2} - \frac{l'(l'+1)}{r_3^2} + k_{\alpha'}^2 \right) u_{\alpha'}^J(r_3) \\ & - 2 \sum_{\alpha''} \langle \alpha'; J | V | \alpha''; J \rangle u_{\alpha''}^J(r_3) \\ & + 2 \sum_{\alpha''} \int_0^\infty K(\alpha', \alpha''; J | r_1, r_3) u_{\alpha''}^J(r_1) dr_1 = 0, \end{aligned} \quad (11)$$

where $k_{\alpha'}^2$ is the channel wave number given by

$$k_{\alpha'}^2 = k_{\alpha'}^2 - [j'(j'+1) - j(j+1)]/I - \nu_0(v' - v), \quad (12)$$

where I is the moment of inertia of the rigid rotator, and ν_0 is the vibrational frequency. The direct interaction potential is given by

$$\begin{aligned} \langle \alpha'; J | V | \alpha''; J \rangle &= \int \mathcal{Y}_{Jj}^{M*}(\hat{r}_3, \vec{s}) Z(v'j'|s) V(\vec{r}_1, \vec{r}_2, \vec{r}_3; \vec{s}) \\ &\times |\phi_0(\vec{r}_1, \vec{r}_2, \vec{s})|^2 \mathcal{Y}_{Jj}^{M''}(\hat{r}_3, \vec{s}) Z(v''j''|s) \\ &\times d\vec{r}_1 d\vec{r}_2 d\vec{r}_3 d\vec{s}. \end{aligned} \quad (13)$$

The exchange terms are contained in the last term on the left-hand side of Eq. (11). If we assume that the wave function for the ground state of the hydrogen molecule is orthogonal to the radial function which describes the motion of the free electron, then only one term contributes to the exchange kernel. Thus, we have

$$K(\alpha', \alpha''; J | r_1, r_3) = \int \mathcal{Y}_{Jj}^{M*}(\hat{r}_3, \vec{s}) Z(v'j'|s) \phi_0(\vec{r}_1, \vec{r}_2, \vec{s})$$

$$\begin{aligned} & \times r_3^{-1} \phi_0(\vec{r}_2, \vec{r}_3, \vec{s}) y_{j,j',l',l''}^M(\hat{r}_1, \hat{s}) Z(v'j''|s) \\ & \times d\hat{r}_1 d\hat{r}_2 d\hat{r}_3 d\vec{s}. \end{aligned} \quad (14)$$

The coupled equations (11) have to be solved subject to the boundary conditions

$$\begin{aligned} u_{\alpha'\alpha}^J(0) &= 0 \\ u_{\alpha'\alpha}^J(r) &\sim_{\infty} \sin(k_{\alpha'\alpha} r - \frac{1}{2}l'\pi) \delta_{\alpha'\alpha} \\ &+ \cos(k_{\alpha'\alpha} r - \frac{1}{2}l'\pi) R^J(\alpha', \alpha), k_{\alpha'\alpha}^2 > 0 \\ &\sim_{\infty} \exp(-|k_{\alpha'\alpha} r|), k_{\alpha'\alpha}^2 < 0, \end{aligned} \quad (15)$$

where the R matrix is related to the T matrix through

$$\underline{T} = 2i \underline{R} (1 - i \underline{R})^{-1}. \quad (16)$$

The elements of the R matrix may be used to obtain the differential cross section for $v_j \rightarrow v'j'$ transitions averaged over all m_j and summed over $m_{j'}$. We obtain

$$\frac{d\sigma}{d\theta}(vj \rightarrow v'j'|\theta) = \frac{\pi(-1)^{j'-j}}{2(2j+1)k_{\alpha\alpha}^2} \sum_{\lambda=0}^{\infty} A_{\lambda} R_{\lambda}(\cos\theta), \quad (17)$$

where A_{λ} coefficients are defined by Arthurs and Dalgarno,⁸ and a factor 2π from integration over azimuthal angle has been included. The expression for the total cross section is

$$\sigma(vj \rightarrow v'j') = \frac{\pi}{(2j+1)k^2} \sum_{\alpha} \sum_{\alpha'} (2J+1) |T^J(\alpha, \alpha')|^2, \quad (18)$$

where l and l' take on all values consistent with j, j' , and J .

III. e - H_2 POTENTIALS

The direct-interaction potential for the e - H_2 system given by Eq. (13) may be written

$$\begin{aligned} \langle \alpha'; J | V | \alpha''; J \rangle &= \int y_{j,j',l',l''}^M(\hat{r}_3, \hat{s}) Z(v'j'|s) \bar{V}(\vec{r}_3, \vec{s}) \\ &\times y_{j,j',l',l''}^M(\hat{r}_3, \hat{s}) Z(v''j''|s) d\hat{r}_3 d\vec{s}, \end{aligned} \quad (19)$$

where

$$\bar{V}(\vec{r}_3, \vec{s}) = \langle \phi_0 | V(\vec{r}_1, \vec{r}_2, \vec{r}_3; \vec{s}) | \phi_0 \rangle. \quad (20)$$

This potential, which has been averaged over the electronic coordinates of the molecule, may be represented by

$$\bar{V}(\vec{r}_3, \vec{s}) = \sum_{\lambda} v_{\lambda}(r_3, s) R_{\lambda}(\hat{r}_3 \cdot \hat{s}). \quad (21)$$

Thus, the direct matrix element may be reduced by

$$\langle \alpha'; J | V | \alpha''; J \rangle = \sum_{\lambda} f_{\lambda}(j'l', j''l'') \langle v' | v_{\lambda}(r_3, s) | v'' \rangle, \quad (22)$$

where the f_{λ} coefficients are given by Arthurs and

Dalgarno,⁸ and we have

$$\langle v' | v_{\lambda}(r_3, s) | v'' \rangle = \int Z(v'j'|s) v_{\lambda}(r_3, s) Z(v''j''|s) ds. \quad (23)$$

The dependence of this matrix element on rotational quantum j is omitted, since we ignore the j -dependence of the nuclear wave functions Z . We may then write Eq. (3) in the form

$$\left(\frac{d^2}{ds^2} + 2\mu[E_{v_0} - \epsilon(s)] \right) Z(v_0|s) = 0, \quad (3')$$

where μ is the reduced mass of the hydrogen molecule. The electronic energy $\epsilon(s)$ is given by Kolos and Wolniewicz,¹⁰ and we solve Eq. (3a) to obtain the vibrational wave functions which are required in Eq. (23).

A. Short-Range Potential

We use the wave function given by Wang¹¹ to represent the ground state of H_2 . If we ignore the cross terms in $|\phi_0|^2$ in calculating the electron-molecule interaction potential, we may write¹

$$\bar{V}(\vec{r}_3, \vec{s}) = U(|\vec{r}_3 + \frac{1}{2}\vec{s}|) + U(|\vec{r}_3 - \frac{1}{2}\vec{s}|), \quad (24)$$

where

$$U(r) = [r^{-1} + z(s)] \exp[-2z(s)r]. \quad (25)$$

The effective nuclear charge $z(s)$ is a function of the internuclear separation s , and has been calculated by Rosen.¹² A fit to Rosen's results yields

$$z(s) = 1 + (0.863 - 0.319s) \exp(-0.641s). \quad (26)$$

We expand (24) in a series of Legendre polynomials and obtain

$$v_{\lambda}(r_3, s) = (2\lambda + 1) \int_{-1}^1 U(r) P_{\lambda}(t) dt, \quad (27)$$

where

$$r = (r_3^2 + s^2 + 2r_3 s t)^{1/2}. \quad (28)$$

Solutions of Eq. (3) are combined with expression (27) in Eq. (23) to yield the coefficients of the short-range interaction potential, averaged over the internuclear distance.

Values for $\langle v | v_0(r_3, s) | v' \rangle$ and $\langle v | v_2(r_3, s) | v' \rangle$ are given in Figs. 1 and 2, respectively, for $v, v' = 0, 1, \text{ and } 2$. Circles represent the short-range potential calculated by Lane and Geltman,¹³ who used the Wang function at equilibrium internuclear separation and so did not average over s . Curves (A), (C), and (F) represent averages over $v(=v') = 0, 1, \text{ and } 2$, respectively. For these curves, as the vibrational quantum is increased, the potential wells become less deep and the minima occur at smaller values of r_3 . This is a consequence of the potential $v_{\lambda}(r_3, s)$ increasing with increasing

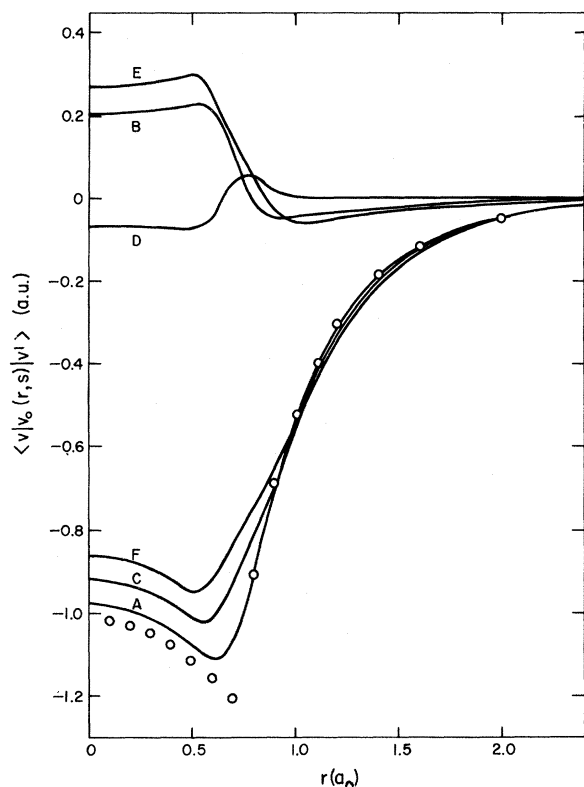


FIG. 1. Spherical part of the short-range potential averaged over initial v and final v' vibrational states. Curves (A) $v=0, v'=0$; (B) $v=0, v'=1$; (C) $v=1, v'=1$; (D) $v=0, v'=2$; (E) $v=1, v'=2$; (F) $v=2, v'=2$. The open circles correspond to the unaveraged potential of Lane and Geltman, (Ref. 13).

s for $r_3 < 0.6a_0$, and of the weighting in integral (23) provided by the factor $Z(v'0|s)^2$. For $v'=0$, this factor has a maximum at $s=1.43a_0$; for $v'=1$ maxima occur at 1.24 and 1.72 a_0 , and at 1.15, 1.51, and 1.93 a_0 for $v'=2$. Thus, as v' increases, the first maximum in the factor Z^2 shifts to smaller s and the larger values of $v_\lambda(r_3, s)$ are weighted less. For $r_3 > 1.0a_0$, $v_\lambda(r_3, s)$ decreases with increasing s and so curve (A) is less attractive than curve (F).

Curves (B), (D), and (E) represent averages $\langle 0||1 \rangle$, $\langle 0||2 \rangle$, and $\langle 1||2 \rangle$, respectively. Averaged potentials over vibrational levels which differ by $\Delta v=1$ are repulsive for small values of r_3 , and attractive for $r_3 > 0.8a_0$. For curve (D), the averaged potential is repulsive for $0.65 < r_3 < 2.0a_0$. This barrier may be important in calculation of $v=0-2$ vibrational cross sections and may lead to values which are much lower than experiment.

B. Long-Range Potential

Asymptotically, our choice of molecular wave function results in exponential behavior for all

the averaged short-range potential. In order to have the correct asymptotic behavior for the interaction potential, we add long-range, electron-quadrupole, and polarization interactions to the short-range portions.

The quadrupole interaction may be represented by¹³

$$v_2^Q(r_3, s) = -Q(s)r_3^{-3}\{1 - \exp[-(r_3/r_0)^6]\}, \quad (29)$$

where the quadrupole moment Q is a function of internuclear distance and $r_0=1.8a_0$. This choice for r_0 is consistent with the general behavior of the unperturbed $e\text{-H}_2$ potential as calculated at the equilibrium internuclear separation by Dalgarno and Henry.¹⁴

An effective adiabatic polarization potential may be represented by¹⁵

$$v_0^P(r_3, s) = -[\alpha_0(s)/2(r_3^2 + r_1^2)^2]\{1 - \exp[-(r_3/r_a)^3]\}, \quad (30)$$

$$v_2^P(r_3, s) = \begin{cases} -[\alpha_2(s)/2(r_3^2 - r_2^2)^2]\{1 - \exp[-(r_3/r_b)^4]\}, & r_3 \geq 0.5 \\ 0, & r_3 < 0.5 \end{cases} \quad (31)$$

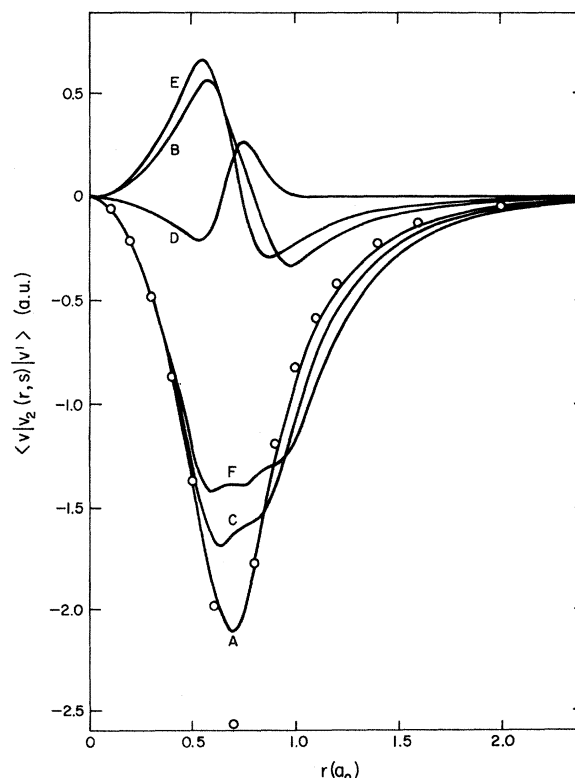


FIG. 2. Anisotropic part of the short-range potential averaged over vibrational states v and v' ; Curves (A)–(F) and open circles as in Fig. 1.

where the spherically symmetric and anisotropic polarizabilities α_0 and α_2 are functions of internuclear distance. Parameters r_1 , r_2 , r_a , and r_b are 1.22, 0.1, 1.7, and $2.0\alpha_0$, respectively, and are chosen to fit the nonpenetrating scaled polarization potentials calculated at the equilibrium internuclear separation by Lane and Henry.¹⁵

We assume that the long-range interactions are in the form

$$v_\lambda(r_3, s) = G_\lambda(s)g_\lambda(r_3). \quad (32)$$

Then, Eq. (23) reduces to

$$\langle v | v_\lambda^L(r_3, s) | v' \rangle = \langle v | G_\lambda | v' \rangle g_\lambda(r_3). \quad (33)$$

Table I gives factors $\langle v | v' \rangle$ for the quadrupole moment and polarizabilities which have been calculated from the functions given by Kolos and Wolniewicz,¹⁰ and Wolniewicz,¹⁶ respectively.

For the exchange kernel (14), we employ the expression calculated by Henry and Lane¹⁷ who used the five-term single-center Huzinaga¹⁸ function to describe the H_2 molecule. If we neglect the dependence of the molecular function on s , then the exchange term reduces to that given in Ref. 17, Eq. (24), times a scaling factor $\langle v' | v'' \rangle$, where

$$\langle v' | v'' \rangle \equiv \delta_{v'v''} = \begin{cases} 1, & \text{if } v' = v'' \\ 0, & \text{if } v' \neq v'' \end{cases}. \quad (34)$$

IV. RESULTS AND DISCUSSION

We calculate cross sections for simultaneous rotational and vibrational excitation of molecular hydrogen by electron impact by solving the set of coupled equations (11) subject to the asymptotic conditions (15). The numerical solution is obtained by using Numerov's method to integrate the equations outwards and inwards, with subsequent matching to obtain a final continuous solution. The asymptotic method of Burke and Schey¹⁹ is used to determine the R matrix from the function $u_{\alpha', \alpha}^J(r)$. A combination of these methods has been outlined by Smith, Henry, and Burke.²⁰ Since there is no significant change in results for cross sections as a function of energy, we ignore values

of $l' > 5$, thus reducing the number of channels involved in Eq. (11). However, to ensure that the expansion in Eq. (17) converges at all angles for the differential cross sections, we include values $l' \leq 8$ for certain energies.

In order to illustrate some of the features of the problem, we consider an electron incident on a hydrogen molecule which is initially in its $v=0$, $j=1$ state, and examine cross sections for $v=0-1$, $\Delta j=0$, which we calculate in several approximations. For all the curves of Fig. 3, exchange terms and a long-range quadrupole term are included in the interaction potential in the manner described in Sec. III. For curves (A), (B), and (C) we have included $v''=0, 1$ and $j''=1, 3$ in the summation over α'' in Eq. (11). Curve (A) results when we assume that there is coupling between $v'=0$ and $v''=1$ states for both short-range interaction and long-range polarization terms. However, to obtain curve (B), we assume vibrational coupling of polarization terms while omitting the coupling between $v'=0$ and $v''=1$ states for short-range terms. They are given by the Wang potential of Ref. 17 times a factor $\delta_{v'v''}$. Similarly, curve (C) results when we ignore off-diagonal vibrational coupling terms for the polarization interaction but retain the corresponding short-range terms. Curves (D) and (E) are obtained when we include $v''=0, 1$, $j''=1$ and $v''=0, 1, 2$, $j''=1$, respectively, in the summation over α'' , and the same potentials are used as in curve (A).

An analysis of individual contributions to the vibrational-excitation cross section shows that the dominant contribution comes from incident and final p -wave electrons.²¹ The total angular momentum J values which have $l=1$ associated with them contribute 99% of the cross section in the energy range $1.0 < E < 10.0$ eV. Due to the centrifugal barrier, slow incident p electrons will not penetrate the inner regions of the molecule and so only the outer portion ($r > 1.0\alpha_0$) of the potential is important for the energy range under consideration. From curve (B) of Figs. 1 and 2, we note that the short-range interaction is attractive for $r > 1.0\alpha_0$. If we ignore the off-diagonal vibrational coupling terms for the short-range interaction, the electron-molecule interaction will be less strong, and the resulting cross section will be lower than that obtained when all potential terms are retained. Thus in Fig. 3, curve (B) is lower than curve (A). Similarly, the polarization potential is attractive and we expect its omission to yield lower cross sections. As the energy is increased, p -wave electrons will penetrate further into the molecule and the short-range interaction will become more important relative to the long-range polarization terms. Thus,

TABLE I. Asymptotic factors in Eq. (33) averaged over internuclear distance.

v	v'	$\langle v Q v' \rangle$ (ea_0^3)	$\langle v \alpha_0 v' \rangle$ (a_0^3)	$\langle v \alpha_2 v' \rangle$ (a_0^3)
0	0	0.484	5.414	1.349
0	1	0.088	0.739	0.406
1	1	0.536	5.885	1.658
0	2	-0.011	-0.071	-0.0075
1	2	0.123	1.070	0.623
2	2	0.586	6.373	1.995

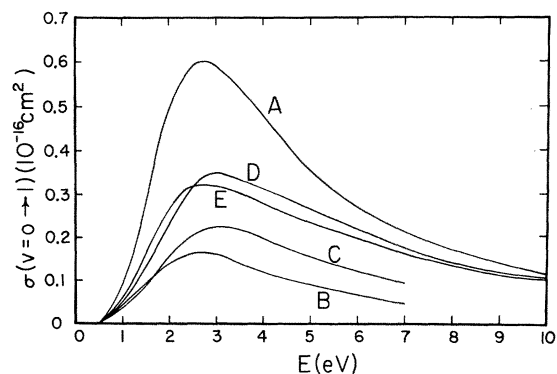


FIG. 3. Pure vibrational cross section for scattering of electrons by H_2 as a function of energy. See text for description of curves (A)–(E).

curve (C) becomes larger than curve (B) as the energy increases.

The effect on vibrational cross sections of coupling between different vibrational and rotational levels can be deduced from comparing curves (A), (D), and (E) of Fig. 3. The greatest change in the $v=0 \rightarrow 1$, $\Delta j=0$ cross section is seen to occur in going from $v''=0, 1, j''=1$, to $v''=0, 1, j''=1, 3$, since there is relatively strong coupling between the rotational levels, and the $j''=3$ state is separated from $j''=1$ in the upper vibrational level by

only 8% of the energy difference between vibrational levels. However, it is not anticipated that further inclusion of higher rotational states would yield significant changes in the cross section. Since the dominant contribution to the pure vibrational cross section comes from $J=0$ and 2, the rotational state $j''=5$ would give rise to coupling with $l''=5$ and $l''=3$ and 5, respectively. The addition of a higher vibrational level changes the $v=0 \rightarrow 1$, $\Delta j=0$ cross section by less than 10%. In this case, the $v''=2$ level is weakly coupled to the $v'=0$ and 1 levels and is well separated in energy from the upper vibrational level.

Figure 4 gives the $v=0 \rightarrow 1$, $\Delta j=0$, pure vibrational-excitation cross section for H_2 as a function of electron impact energy E . For the curves, all direct and exchange terms are included in the manner described in Sec. III. The terms in the summation over α'' which are retained are $v''=0, 1$, and $j''=j, j+2$, where $j=0, 1$, and 2 for curves (A), (B), and (C), respectively. The chief feature of the results given in Fig. 4 is that, for the potentials used in this close-coupling calculation, the pure vibrational cross section depends on the initial rotational state of the molecule. This appears to be due to the different ways in which the spherically symmetric and anisotropic portions of the interaction potential $v_0(r, s)$ and $v_2(r, s)$ are combined for the various rotational states.

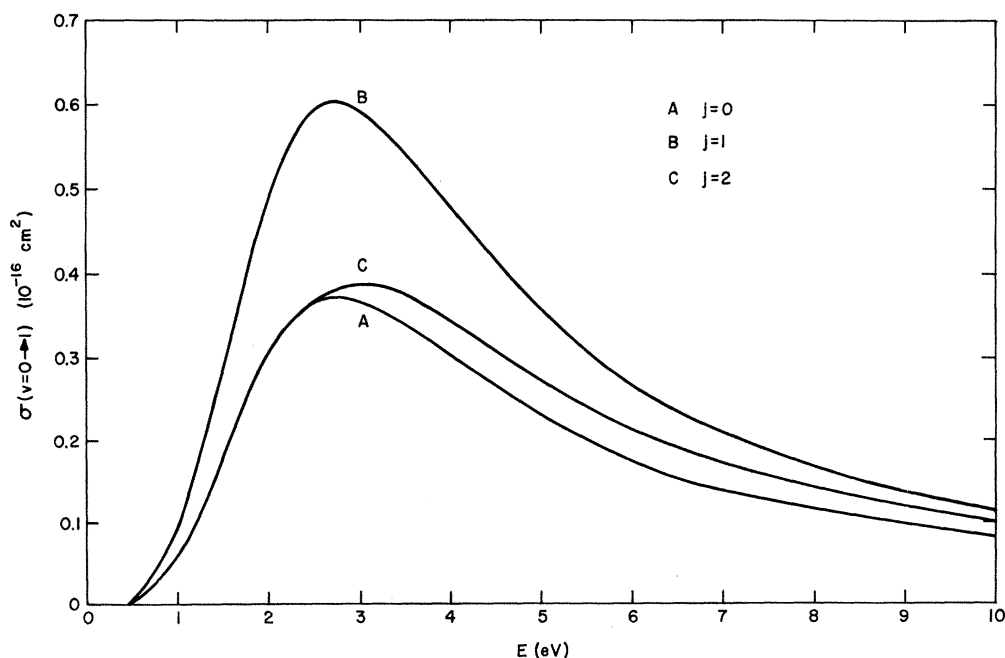


FIG. 4. Pure vibrational cross section for scattering of electrons by H_2 as a function of energy. Curves (A), (B), and (C) represent results obtained when the initial rotational state is $j=0, 1$, and 2, respectively.

To illustrate this point, let us consider only incident and final p -wave electrons interacting with an H_2 molecule which is in rotational state j . We will assume that there is no change in rotational state due to the collision. In the distorted-wave approximation, the vibrational-excitation cross section is proportional to the square of the matrix element $\langle u_{v_j} \bar{V} u_{v_j} \rangle$, where $\bar{V}(r) = \langle v | v_0(r, s) + f_2 v_2(r, s) | v \rangle$. Wave functions $u_{v_j}(r)$ and $u_{v_j}(r)$ depend on $\langle v | v_0(r, s) + f_2 v_2(r, s) | v \rangle$ and $\langle v' | v_0(r, s) + f_2 v_2(r, s) | v' \rangle$, respectively; i.e., they represent the radial motion of p electrons under the influence of the corresponding vibrationally averaged interaction potential. If the molecule is initially in rotational state $j=0$, only total angular momentum $J=1$ can lead to $l=1$, and in this case $f_2=0$. If the initial rotational state is $j=1$, then the values of J are 0 and 2, and those of f_2 are $\frac{2}{5}$ and $\frac{1}{25}$, respectively. Thus, in this particular approximation, the cross sections are seen to depend on the value of the initial rotational state.

However, in our case, we use the close-coupling approximation which reduces to the distorted-wave approximation in the weak-coupling limit. Further, since we do not restrict the orbital angular momentum to only p waves, the situation is actually much more complicated than the case used as an illustration.

Let us consider a hydrogen molecule which is initially in its $v=0, j=1$ state and include $v''=0, 1$ and $j''=1, 3$ in the expansion over α'' in Eq. (11); then cross sections for four processes may be calculated. These are elastic scattering $v=0 \rightarrow 0, \Delta j=0$; rotational excitation $v=0 \rightarrow 0, j=1 \rightarrow 3$; vibrational excitation $v=0 \rightarrow 1, \Delta j=0$; and simultaneous rotational-vibrational excitation $v=0 \rightarrow 1, j=1 \rightarrow 3$.

An experiment has been performed by Crompton *et al.*²² in an attempt to corroborate the above suggestion that the vibrational cross section depends on the initial rotational state. They measured the drift velocity of electrons in normal and parahydrogen at 77 °K at energies far away from threshold.

TABLE II. Cross sections in units of 10^{-18} cm^2 for the following processes: A, $\sigma(v=0 \rightarrow 1, j=0 \rightarrow 0)$; B, $\alpha(v=0 \rightarrow 1, j=0 \rightarrow 2)$; C, $\sigma(v=0 \rightarrow 1, j=1 \rightarrow 1)$; D, $\sigma(v=0 \rightarrow 1, j=1 \rightarrow 3)$.

$E(\text{eV})$	A	B	A+B	C	D	C+D
1.0	0.06	0.05	0.11	0.09	0.03	0.12
2.0	0.30	0.34	0.64	0.49	0.21	0.69
3.0	0.37	0.46	0.83	0.59	0.28	0.87
4.42	0.27	0.35	0.62	0.42	0.21	0.63
5.5	0.20	0.26	0.46	0.31	0.16	0.47
7.0	0.14	0.17	0.31	0.21	0.10	0.31
10.0	0.08	0.09	0.17	0.11	0.05	0.17

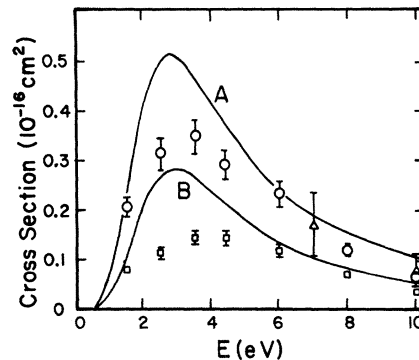


FIG. 5. Pure vibrational cross sections $\sigma(v=0 \rightarrow 1, \Delta j=0)$ and rotational-vibrational cross sections $\sigma(v=0 \rightarrow 1, j=1 \rightarrow 3)$ as a function of energy are given by curves (A) and (B), respectively. Experimental results for corresponding processes obtained by Linder (Ref. 24) are given by open circles and open squares.

They found that to within 0.25%, the relative accuracy claimed in this energy region, the drift velocities are the same in both gases. Energetic swarms lose the same total energy in rotational excitations in both normal and parahydrogen at 77 °K, since the ratio²³ of pure rotational-excitation cross sections $\sigma(j=0 \rightarrow 2)/\sigma(j=1 \rightarrow 3)$ is approximately $\frac{5}{3}$, which is just the inverse of the ratio of threshold energies for these processes. Thus, as the swarm energies are the same in both gases, the total vibrational cross sections are the same. If we interpret the total vibrational cross section as the pure vibrational $\alpha(v=0 \rightarrow 1, \Delta j=0)$ plus the rotational-vibrational ($v=0 \rightarrow 1, \Delta j=2$) cross section, then from Table II, we have that the sum of these cross sections is the same to within 7% for the $j=0$ and $j=1$. Hence, the theoretical results are consistent with experiment. Further, from Table II, at energies far enough away from threshold, the ratio of simultaneous rotational-vibrational excitation cross section (B:D) is approximately 1.63, which we note is very close to the ratio of pure rotational-excitation cross sections. Since the rotational-vibrational cross sections are not equal, it follows that the pure vibrational cross section depends on the initial state of the molecule.

In Fig. 5, curves (A) and (B) represent cross sections for pure vibrational excitation $\sigma(v=0 \rightarrow 1, \Delta j=0)$ and rotational-vibrational excitation $\sigma(v=0 \rightarrow 1, j=1 \rightarrow 3)$ of H_2 as a function of electron impact energy E . Circles and squares denote values for these respective cross sections which have been measured by Linder,²⁴ who used a crossed-beam technique to measure the energy dependence in the range $0.3 < E < 10$ eV and the angular dependence ($0^\circ - 120^\circ$) of the differential cross sections for the above four processes. By extrapolating mea-

surements to 180° , integrating over the angular range, and normalizing his results to the absolute total cross sections of Golden *et al.*,²⁵ Linder obtained cross sections for the different processes in absolute units. For the curves, all direct and exchange terms are included in the manner described in Sec. III. For curve (A) we have taken a weighted average of the results given in Fig. 4. We assumed a relative distribution of initial rotational states to be 13.6 : 67.1 : 19.3 for $j=0, 1$, and 2. This average corresponds to the Boltzmann distribution at room temperature under which condition the experiments of Linder were performed.

For pure vibrational excitation, the present calculations have a maximum in the cross section at $E = 2.8$ eV while the maximum in experimental cross section is at 3.5 eV. The ratio of these maxima is 1.5. For simultaneous rotational-vibrational excitation the maxima in theoretical and experimental cross sections are at 3.0 and 4.0 eV, respectively, and their ratio is 1.9. The ratio of the maximum of our total cross section to that of Golden *et al.*²⁵ is 1.2, and so, if the results of Linder were normalized to our total cross sections, the discrepancy in magnitude of the pure vibrational and rotational-vibrational cross sections would be decreased. However, the calculated cross sections would still lie well outside the experimental error limits, particularly for energies in the range $2.0 < E < 5.0$ eV. This may be due to the manner in which polarization effects are included in this calculation. We have assumed that the long-range potential can be factored as in Eq. (32). If, however, the vibrational average produces long-range potentials which are similar in shape to those given in Figs. 1 and 2, then, as a result, we overestimate the polarization potential, and thus obtain cross sections which are too large when compared with experiment.

Total vibrational cross sections $\sigma(v=0 \rightarrow 1)$ and $\sigma(v=0 \rightarrow 2)$ are compared with experiment in Fig. 6. Curve (A) is obtained when we assume a room-temperature Boltzmann distribution of initial rotational states for normal hydrogen, and represents $\sigma(v=0 \rightarrow 1)$. Circles represent the experimental results of Ehrhardt *et al.*,²⁶ which are identical to those of Linder,²⁴ and results from another scattering experiment by Trajmar *et al.*²⁷ are given by squares. Electrostatic-energy-analyzer studies of Schulz²⁸ are presented as triangles, and diamonds denote cross sections deduced by Engelhardt and Phelps²⁹ from analysis of transport data. The dashed curves near threshold energies represent the results of Burrow and Schulz³⁰ who used the trapped-electron method to measure the slopes of the vibrational cross sections. They obtained 4.3×10^{-17} and 7.2×10^{-19} cm² eV⁻¹ for $v''=1$ and 2, respectively.

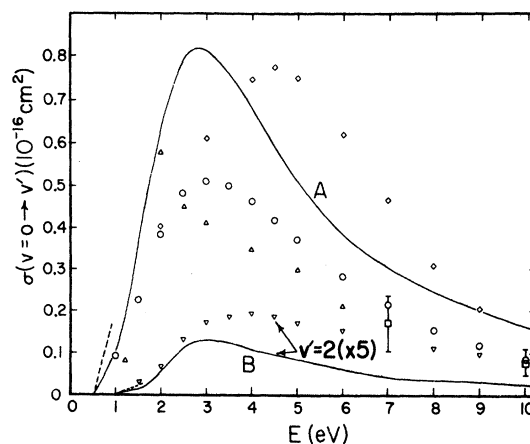


FIG. 6. Total vibrational cross sections $\sigma(v=0 \rightarrow 1)$ and $\sigma(v=0 \rightarrow 2)$ as a function of energy are given by curves (A) and (B), respectively. Experimental results for $\sigma(v=0 \rightarrow 1)$ are given by: O, Ehrhardt *et al.* (Ref. 26); \square , Trajmar *et al.* (Ref. 27); \triangle , Schulz (Ref. 28); \diamond , Engelhardt and Phelps (Ref. 29); ---, Burrow and Schulz (Ref. 30). Experimental results for $(v=0 \rightarrow 2)$ are given by: ∇ , Ehrhardt *et al.* (Ref. 26); ---, Burrow and Schulz (Ref. 30).

Curve (B) is obtained when we include $v''=0, 1, 2, j=1$ in the summation over α'' in Eq. (11), and all direct and exchange terms are included in the interaction potential. The inverted triangles denote experimental results of Ehrhardt *et al.*²⁶ Note that vibrational cross sections for $v=0 \rightarrow 2$ have been multiplied by a factor of 5. In Fig. 3, it was shown that cross sections for one vibrational quantum change were *significantly* affected by inclusion of the $j''=3$ level in the expansion of the total wave function, and a similar effect on $\sigma(v=0 \rightarrow 2)$ may occur if we include $v''=0, 1, 2$ and $j=1, 3$, in the summation over α'' . Further, simultaneous rotational-vibrational cross sections are included in the experimental results and this may give an additional explanation as to why the theoretical results are lower than experiment.

Differential cross sections for $v=0 \rightarrow 1$ vibrational excitation of molecular hydrogen by electron impact are given as a function of angle at $E=10$ eV in Fig. 7. Theoretical curves are calculated with all terms included in the direct and exchange potentials, and $v''=0, 1, j''=j, j+2$ included in summation over α'' . Circles and squares denote experimental results which were obtained from a study of normal hydrogen at room temperature by Ehrhardt *et al.*²⁶ and Trajmar *et al.*,²⁷ respectively. These measurements refer to total vibrational cross sections and have been normalized using the absolute total scattering cross sections obtained by Golden *et al.*²⁵ Curves (A) and (B)

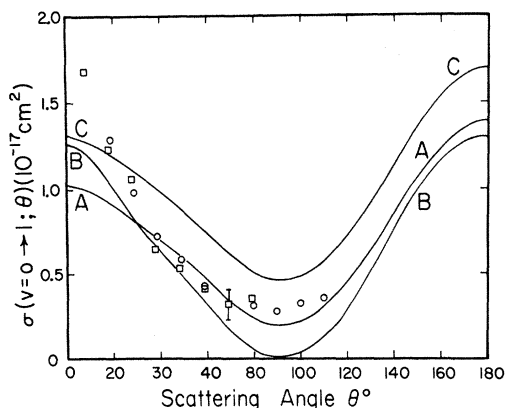


FIG. 7. Differential cross sections for vibrational excitation of H_2 by electron impact, as a function of angle at $E=10$ eV. Curves (A) $v=0 \rightarrow 1$, $\Delta j=0$ for $n-H_2$ at $293^\circ K$; (B) $v=0 \rightarrow 1$, $\Delta j=0$ for $p-H_2$ at $77^\circ K$; (C) $v=0 \rightarrow 1$, ($\Delta j=0 + \Delta j=2$). Experimental results for total vibrational excitation are given by O, Ehrhardt *et al.* (Ref. 26) and \square , Trajmar *et al.* (Ref. 27).

represent present results for pure vibrational excitation of $n-H_2$ at $293^\circ K$ and $p-H_2$ at $77^\circ K$, respectively. We note the difference in angular behavior predicted for these gases. In particular, for the gas with all molecules initially in $j=0$ rotational level, the angular distribution varies approximately as $\cos^2\theta$. The sum of pure vibrational and simultaneous rotational-vibrational cross sections for $n-H_2$ at $293^\circ K$ is given by curve (C). This theoretical curve may be com-

pared with the experimental points. For the angular range $20^\circ < \theta < 120^\circ$, the shape and magnitude of the present results are in good agreement with experiment. However, theory fails to reproduce the large forward peak for low scattering angles.

Figure 8 gives the ratio of pure vibrational ($v=0 \rightarrow 1$, $\Delta j=0$) to simultaneous rotational-vibrational ($v=0 \rightarrow 1$, $\Delta j=2$) cross section for $n-H_2$ at $293^\circ K$ as a function of scattering angle for $E=4.42$ eV. Circles represent measurements of Ehrhardt and Linder.³¹ Curve (A) represents the calculation of Abram and Herzenberg⁶ who used an adiabatic approximation, and curve (B) depicts the present results. Agreement of theory with experiment is poor for small angles but improves with increasing angle. This failure of theory at small angles may be due to the manner in which polarization is included in the present treatment. An analysis of our results shows that the magnitude and shape of low-angle differential cross sections for vibrational excitation is determined primarily by the long-range polarization potential, whereas, the short-range potential is important for large-angle scattering. Thus, relaxation of the assumption that the polarization potential can be factored as in Eq. (32) may lead to improvement between theory and experiment for both integral and differential vibrational-excitation cross sections.

V. SUMMARY

Static-field and electron-exchange effects, a long-range quadrupole, and an effective polarization

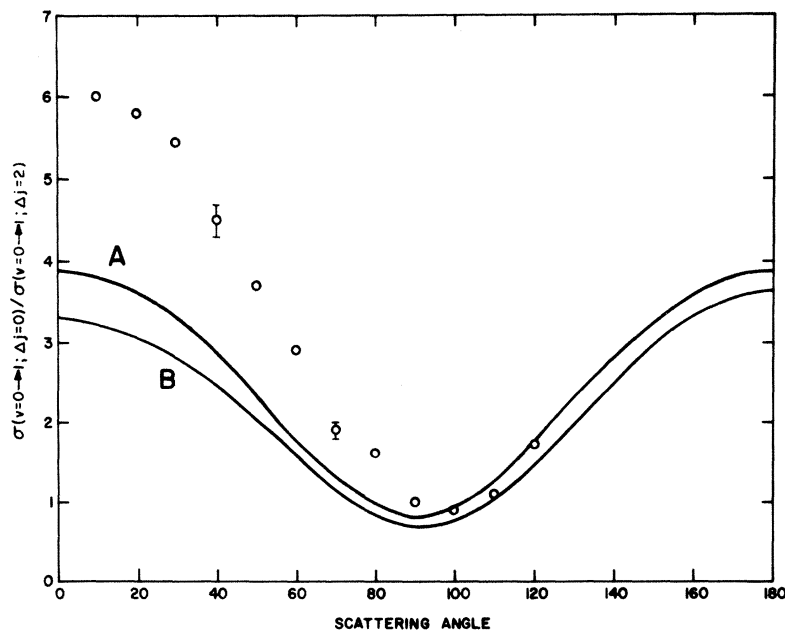


FIG. 8. Ratio of pure vibrational to rotational-vibrational cross section as a function of angle at $E=4.42$ eV. Circles represent measurements of Ehrhardt and Linder (Ref. 31). Curves (A) Abram and Herzenberg (Ref. 6); (B), present results.

potential are included in the e - H_2 interaction. Omission of either the short-range terms or the long-range polarization term causes a decrease by a factor of 2 in the pure vibrational-excitation cross sections over those calculated with all terms retained. Differential scattering cross sections for vibrational excitation are found to be dominated by the polarization potential at small angles, and by the short-range potential at large angles.

For pure vibrational excitation, larger cross sections are obtained when the states $v''=0, 1, j''=1, 3$ are included in the close-coupling expansion, than when state $v''=0, 1, j''=1$ are retained. Inclusion of a higher vibrational level changes the cross section $\sigma(v=0-1, \Delta j=0)$ by less than 10%.

Pure vibrational-excitation cross sections de-

pend on the initial rotational state. Consequently, an experiment which measures scattering of electrons on parahydrogen at 77 °K would obtain smaller cross sections than an experiment on electrons in normal hydrogen at room temperature. However, total vibrational cross sections $\sigma(v=0-1, \Delta j=0) + \sigma(v=0-1, \Delta j=2)$ are almost independent of j . Thus, for example, results of Crompton *et al.*³² and Ehrhardt *et al.*²⁶ should yield the same values for the cross sections since they measure total vibrational excitation of p - H_2 and n - H_2 by electron impact.

ACKNOWLEDGMENTS

We would like to thank Dr. D. K. Gibson, Dr. F. Linder, and Dr. D. G. Truhlar for supplying us with their results prior to publication.

¹T. R. Carson, Proc. Phys. Soc. (London) A67, 909 (1954).

²K. Takayanagi, J. Phys. Soc. Japan 20, 562 (1965); 20, 2297 (1965).

³E. L. Breig and C. C. Lin, J. Chem. Phys. 43, 3839 (1965).

⁴D. G. Truhlar, J. K. Rice, A. Kuppermann, and S. Trajmar, in *Proceedings of the Sixth International Conference on the Physics of Electronics and Atomic Collisions* (MIT Press, Cambridge, Mass., 1969), p. 148; D. G. Truhlar and J. K. Rice, J. Chem. Phys. 52, 4480 (1970).

⁵J. N. Bardsley, A. Herzenberg, and F. Mandl, Proc. Phys. Soc. (London) 89, 321 (1966).

⁶R. A. Abram and A. Herzenberg, Chem. Phys. Letters 3, 187 (1969).

⁷R. W. B. Ardill and W. D. Davison, Proc. Roy. Soc. (London) A304, 465 (1968).

⁸A. M. Arthurs and A. Dalgarno, Proc. Roy. Soc. (London) A256, 540 (1960).

⁹H. S. W. Massey, Phil. Mag. 4, 336 (1959).

¹⁰W. Kolos and L. Wolniewicz, J. Chem. Phys. 46, 1426 (1967).

¹¹S. C. Wang, Phys. Rev. 31, 579 (1928).

¹²N. Rosen, Phys. Rev. 38, 2099 (1931).

¹³N. F. Lane and S. Geltman, Phys. Rev. 160, 53 (1967).

¹⁴A. Dalgarno and R. J. W. Henry, Proc. Phys. Soc. (London) 85, 679 (1965).

¹⁵N. F. Lane and R. J. W. Henry, Phys. Rev. 173, 183 (1968).

¹⁶L. Wolniewicz, J. Chem. Phys. 45, 515 (1966).

¹⁷R. J. W. Henry and N. F. Lane, Phys. Rev. 183, 221 (1969).

¹⁸S. Huzinaga, Progr. Theoret. Phys. (Kyoto) 17, 162 (1957).

¹⁹P. G. Burke and H. M. Schey, Phys. Rev. 126, 163 (1962).

²⁰K. Smith, R. J. W. Henry, and P. G. Burke, Phys. Rev. 147, 21 (1966).

²¹The l th partial wave refers to the orbital angular momentum of the scattered electron with respect to the center-of-mass system of the molecule.

²²R. W. Crompton, D. K. Gibson, and A. G. Robertson (private communication).

²³E. S. Chang and A. Temkin, Phys. Rev. Letters 23, 399 (1969).

²⁴F. Linder, in *Proceedings of the Sixth International Conference on the Physics of Electronic and Atomic Collisions* (MIT Press, Cambridge, Mass., 1969), p. 141.

²⁵D. E. Golden, H. W. Bandel, and J. A. Salerno, Phys. Rev. 146, 40 (1966).

²⁶H. Ehrhardt, L. Langhans, F. Linder, and H. S. Taylor, Phys. Rev. 173, 222 (1968).

²⁷S. Trajmar, J. K. Rice, D. G. Truhlar, A. Kuppermann, and R. T. Brinkmann, in *Proceedings of the Sixth International Conference on the Physics of Electronic and Atomic Collisions* (MIT Press, Cambridge, Mass., 1969), p. 87.

²⁸G. J. Schulz, Phys. Rev. 135, A988 (1964).

²⁹A. G. Engelhardt and A. V. Phelps, Phys. Rev. 131, 2115 (1963).

³⁰P. D. Burrow and G. J. Schulz, Phys. Rev. 187, 97 (1969).

³¹H. Ehrhardt and F. Linder, Phys. Rev. Letters 21, 419 (1968).

³²R. W. Crompton, D. K. Gibson, and A. I. McIntosh, Australian J. Phys. 22, 715 (1969).